RSC Advances

RSCPublishing

ARTICLE

# Mechanochemical Synthesis of Amorphous Silicon Nanoparticles

Cite this: DOI: 10.1039/x0xx00000x

Anna-Lisa Chaudhary,[a,b*] Drew A. Sheppard,[a] Mark Paskevicius,[a] Martin Saunders[c] and Craig E. Buckley[a]

Received 00th January 2012,
Accepted 00th January 2012

DOI: 10.1039/x0xx00000x

www.rsc.org/

Silicon nanoparticles have been synthesised using mechanochemical ball milling and an inert salt buffer to limit the growth and control the size of the Si particles produced. The solid-liquid metathesis reaction used silicon tetrachloride and lithium with LiCl as the buffer to generate Si nanoparticles. Once the LiCl was removed, X-ray amorphous Si was identified using electron energy loss spectra, at 99 eV and energy filtered transmission electron microscopy. The morphological analysis showed spherical like particles with an average size between 10 – 30 nm depending on the amount of salt buffer phase added to the reactants. This synthesis method can be used to produce very small Si particles in tuneable sizes for a wide range of applications.

## 1. Introduction

Nano dimensional silicon including nanoparticles, nanowires and thin films, have widespread application including the internet and multimedia communication optoelectronic devices, integrated circuits, solar cells, medicine and more recently, hydrogen storage. A major advantage to nanosizing Si comes from its use as a semiconductor material. Nanoscopic Si experiences quantum confinement effects[1, 2], leading to excellent optical and electronic properties. With respect to hydrogen storage, silicon reduces the thermodynamic stability of metal hydrides[3, 4] through the formation of intermetallic metal-silicon alloys upon hydrogen release. Vajo *et. al.*[3] pioneered this field of research using Si to destabilise magnesium hydride (Eqn. 1). Calculations have shown that the Mg-Si-H system has ideal theoretical operating conditions, namely, hydrogen equilibrium pressures of 1 bar at 20 °C and 100 bar at 150 °C with only a minor reduction to hydrogen storage capacity of pure $MgH_2$ from 7.6 wt% to 5 wt%. The Mg-Si-H system has a reduced enthalpy of dehydrogenation from 75.3 kJ $mol^{-1}$, for pure $MgH_2$, to 36.4 kJ $mol^{-1}$ [3]. Despite these promising theoretical properties, the conditions have not yet been achieved experimentally due to extremely slow reaction kinetics.

Eqn. 1 $$2MgH_2 + Si \rightarrow Mg_2Si + 2H_2$$

Several attempts have been made in the past to overcome the reaction kinetic limitations in the Mg-Si-H system including reducing diffusion distances by using smaller particle sizes and introducing defects[3, 5]. Bystrzycki *et. al.*[6] showed that a reduction of diffusion distances and an increase in surface area using nanoscale materials significantly influenced reaction rates. Bystrzycki *et. al.*[6] ball-milled a stoichiometric mixture of $MgH_2$-Si to achieve a reduction in crystallite size to less than 40 nm for both reactants with a mean particle size of 0.5 µm. Diffusion of Si at low temperatures is expected to be very slow and will inevitably control the reaction between $MgH_2$ and Si. Bystrzycki *et. al.*[6] proved there was no significant desorption below 200°C and only a release of 3.4 wt% after 3 hours at 250°C. Similarly, another study that ball-milled these two components showed only 0.03% hydrogen release at 150°C over a 24 hour period with the majority of the hydrogen desorbing at temperatures between 250 and 300°C[5]. These studies indicate that a reduction in crystallite size to the nanoscale level is not enough to overcome reaction kinetic barriers. Particle size has a dominant influence on the reaction kinetics[6, 7], therefore, the focus of this current study is to synthesise extremely small Si particles (~ 10 nm) to enhance the diffusion rate of Mg bonding with Si to form $Mg_2Si$ and release $H_2$.

A promising nanoparticle synthesis technique currently being used for hydrogen storage materials is mechanochemical milling[8, 9]. This technique is a high energy, batch process that uses a mechanically assisted chemical reaction. An example of large scale synthesis of Si nanoparticles was investigated by Lam *et. al.*[10]. The thermodynamics combined with slow reaction kinetics is a problem for this method of Si synthesis as it took an impractical length of time to complete, 7 to 10 days.

An alternative method for nanoparticle production is mechanochemical ball-milling within a soluble salt matrix[11]. This method allows for the control of particle size formation by adjusting the amount of salt added to the initial reactants. The objective is to balance the amount of salt added in order to complete the reaction as well as obtain the smallest particle sizes.

The hypothesis of improved reaction kinetics through small particles size is explored in this study by synthesising Si nanoparticles *via* solid-liquid mechanochemical ball-milling.

## 2. Experimental

Due to the air and moisture sensitivity of the chemicals, all sample handling was undertaken in an argon glovebox. The automatic gas purifier unit maintained low oxygen ($O_2$ < 1 ppm) and moisture ($H_2O$ < 1 ppm) levels to avoid sample contamination and limit any reactions with either $O_2$ or $H_2O$.

Materials were synthesized using a 316 stainless steel (SS 316) custom made ball milling canister[12] (internal chamber volume of 650 $cm^3$) set onto a Glen Mills Turbula T2C Shaker-Mixer. Equal numbers of 7.9 mm and 12.7 mm diameter SS 316 balls were used to obtain the correct ball to powder ratio. All milling was done in argon atmosphere at room temperature at a rotation speed of 160 rpm. Initially, stoichiometric ratios of $SiCl_4$ (Sigma Aldrich, 99.998 %) and Li (Sigma Aldrich, 99.9 %) were ball milled with a ball to powder (BTP) ratio of 90:1 over a 24 h period without adding any LiCl as a buffer agent to the reactants. Another sample was also prepared using LiCl (Sigma Aldrich, > 99 %) as a buffer agent to control the size of Si during its formation. LiCl was added to the reaction with a LiCl to Si ratio of 10:1 based on the final product of Si volumes. Pre-milling the solid reagents (Li with LiCl) before the reduction reaction is undertaken aids in the production of smaller particles during mechanochemical ball milling[13]. Therefore, the sample that contained the LiCl buffer had a stoichiometric amount of $SiCl_4$ added to the powders after 3 h pre-milling before milling for a further 24 h.

The brown Si particles were separated from the LiCl by solvent extraction using tetrahydrofuran (THF, Anhydrous 99.9 with 250 ppm BHT inhibitor, Sigma Aldrich)[14]. This solvent was chosen to 'wash' the LiCl from the Si nanoparticles as it was able to dissolve the LiCl whilst remaining relatively inert to the silicon nanoparticles. The washed (3 times) particles were placed on a single silicon crystal low background dome holder for XRD analysis.

X-ray diffraction (XRD) data was taken using a Bruker D8 Advance (Germany, $CuK_\alpha$, $\lambda$ = 1.5418 Å) X-ray diffractometer in a Bruker supplied airtight, specimen dome holder to avoid exposure to air and moisture. A JEOL 3000F transmission electron microscope (TEM) with a field emission gun (FEG) at 300 keV was used for TEM measurements including electron energy loss spectra (EELS) and energy filtered TEM. Samples for TEM were prepared by suspending the Si nanoparticles in toluene (anhydrous 99.8 %, Sigma-Aldrich) in a sealed vial and ultrasonicating in a water bath for 30 minutes. This solution was added dropwise to a 200 mesh copper grid with holey carbon film. The TEM grids and were exposed to air for a few minutes when loading into the instrument. A Zeiss Neon 40EsB was used for high resolution Scanning Electron Microscopy (SEM). SEM sample preparation was similar to that of the TEM however aluminium stubs were used rather than a copper grid. Small Angle X-ray Scattering (SAXS) was performed on a laboratory Bruker NanoSTAR SAXS instrument (Germany). Borosilicate capillaries (Charles Supper, Germany) were loaded in an Ar atmosphere and sealed to prevent $O_2$ or $H_2O$ contamination. A 65 cm sample-detector distance was used with a copper anode X-ray tube ($\lambda$ = 1.5418 Å) and data was collected for 3 h. The usable *q*-range was 0.014 to 3 $Å^{-1}$. SAXS data was adjusted onto absolute scale using the calibration standard S-2907 provided by the Oak Ridge National Laboratory.[15]

## 3. Results and Discussion

Nanoparticle synthesis was undertaken using mechanochemical ball milling in this study because of its versatility and ability to form small nanoparticles[8]. A liquid-solid reaction pathway was utilised for the synthesis of silicon nanoparticles *via* mechanochemical ball milling (Eqn. 2). Thermodynamic feasibility was determined using *HSC Chemistry* (Outotech Research). It was found that the reaction was thermodynamically favourable based on the large negative value for the Gibbs free energy value ($\Delta_r G_{298K} = -910$ kJ $mol^{-1}$). Inert LiCl, added to the starting reagents, was used as a buffer phase to limit the growth of Si particles as they form, thus controlling their size.

Eqn. 2 $$SiCl_4 + 4Li \rightarrow Si + 4LiCl$$

X-ray diffraction data from the as-synthesised samples with and without buffer are shown in Fig. 1 (A) (i) and (iii). The reactions go to completion with no reactants present in the diffractograms. After washing, XRD no longer detected any LiCl in the samples with and without buffer (Fig. 1 (A) (iv) and (ii)) indicating that washing was successful. Also, XRD did not show any trace of residual reactants after washing. In fact, there was no evidence of crystalline Si in the diffractograms either (Fig. 1 (A) (ii) and (iv)) indicating that the product was X-ray amorphous.

The production of amorphous Si as a brown powder[16] is also an indication of the lack of crystalline structure, as crystalline Si has a metallic luster and is greyish in colour.[16] Amorphous silicon typically presents broad halos centered at 28° and 50° $2\theta$ in an XRD pattern[17]. XRD analysis in a PMMA air-tight dome prevented the detection of these halos so instead 300 nm crystalline aluminium foil was used to cover and protect the sample during XRD analysis.

Fig. 1 (B) shows the XRD pattern of Si (synthesised without buffer) covered by Al foil and also the blank Al foil pattern. It should also be noted that Fig. 1 (B) (i) shows a peak at 32° $2\theta$ that can be attributed to a $LiCl{\cdot}H_2O$ complex. LiCl is extremely hygroscopic and any trace amounts of LiCl remaining from the

 

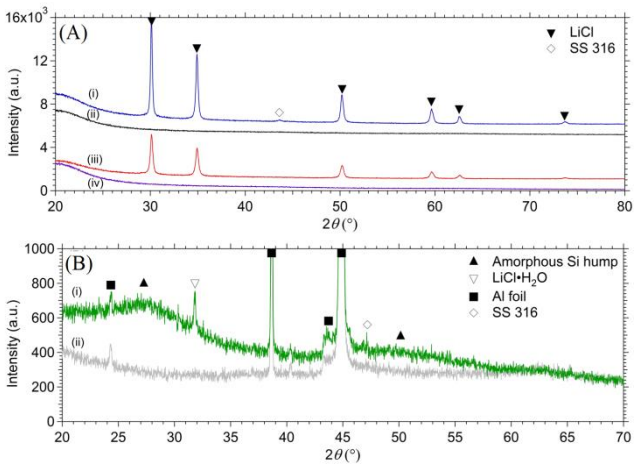


Fig. 1: (A) XRD diffractograms with PMMA amorphous hump at 20° 2$\vartheta$ (i) 24 h reaction time, 90:1 BTP ratio no buffer (ii) Sample (i) washed with THF (iii) 24 h reaction time, 90:1 BTP ratio with 10:1 buffer to product (Si) ratio (iv) Sample (iii) washed with THF. (B) XRD of (i) Washed Si nanoparticles with Al foil barrier (ii) Al foil barrier, no sample.

initial reaction react with $H_2O$ in air that can slowly permeate through the very thin Al foil. Trace amounts of the milling media, stainless steel 316 (SS 316) were also detected.

The XRD data of the washed sample under foil clearly shows two amorphous halos, one centred around 28° and the other at 50° 2$\theta$, in agreement with the positions for amorphous Si [17]. Therefore, it can be concluded that amorphous Si particles were synthesised using mechanochemical ball milling. The formation of an amorphous material is not uncommon during mechanochemical ball milling and has been shown in a number of studies synthesising different products[17-19]. Amorphicity can occur as a result of particles being strained to a critical stress level (i.e. during milling) where the crystal structure is deformed and there is no longer any long-range crystalline order.

In an attempt to crystallize the particles synthesised, two samples were heated to 475°C for 18 h, one sample in the LiCl (that is prior to washing with THF) and the other after washing with THF. According to Poffo *et. al.*[20] amorphous Si particles undergo crystallization at 451°C when heated at a rate of 10°C $min^{-1}$. Another study showed that at a faster heating rate (40°C $min^{-1}$), this crystallization transition was observed at 660°C.[19] However, in both studies, the existence of $O_2$ contamination could not be completely ruled out and this was discussed in Poffo *et. al.*[20] as the reason for the large discrepancy between the two values. It was assumed that there was little or no $O_2$ contamination in the synthesised particles for this study and this will be discussed further in in the results from the Electron Energy Loss Spectroscopy (EELS) data. The XRD showed that Si did not undergo crystallization at 475°C as there was still no evidence of crystalline Si. The sample cell was made from SS 316 and has a temperature rating of 537°C (Swagelok, Australia) therefore higher annealing temperatures were not safely achievable.

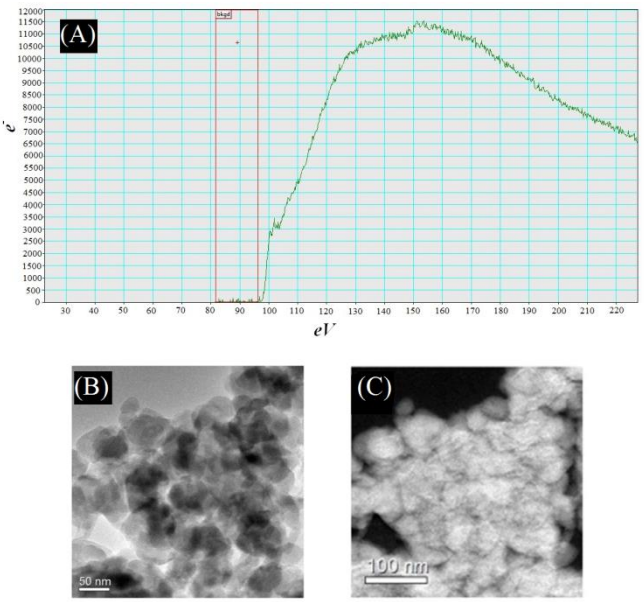


Fig. 2: Washed Si synthesised without buffer: (A) Si EELS spectrum of the 99 eV Si-$L_{2,3}$ edge (pure Si)[21]. (B) TEM micrograph (C) Si EFTEM map.

EELS was used to confirm the presence of the amorphous Si nanoparticles. Unlike XRD that relies on the diffraction of crystalline samples to produce a phase identifying pattern, EELS uses inelastic electron scattering to measure the energy loss from the electron beam after transmission through the sample. The energy loss information can identify elements present in the sample as well as give bonding information. When a spectrum is collected from the detector, K-, L- or M-edges appear depending on which core electrons are present in the atom. Pure Si has a K-edge at 1839 eV and an $L_{2,3}$-edge at 99.2 eV[21]. Fig. 2 (A) shows the background subtracted EELS spectrum of the Si $L_{2,3}$-edge from the washed sample (synthesised without buffer). When silicon is oxidised the $L_{2,3}$-edge typically moves to higher energy (~ 106 eV[21]). Therefore the energy of the Si $L_{2,3}$-edge is characteristic of silicon metal, demonstrating the purity of the as-synthesised sample.

In order to characterise the structure of the sample, a map of the elements was generated using Energy Filtered TEM (EFTEM). This method uses the energy loss information from EELS to produce an elemental image[22]. This is done by acquiring images at energy values immediately before and after the EELS edge, in this case 99 eV. The pre-edge data is used to fit and remove a background from the post-edge data, obtaining an image of the element distribution. Fig. 2 (B) shows the original TEM image of THF washed particles without buffer (from Eqn. 2) and the corresponding EFTEM image of Si (Fig. 2 (C)). The Si map correlates well with the TEM image suggesting that Si not $SiO_2$ was present. Combined with the XRD results this indicates that the mechanochemical synthesis method without buffer has formed nanoparticles (20 – 60 nm measured from Fig. 2 (B)) of amorphous Si metal.

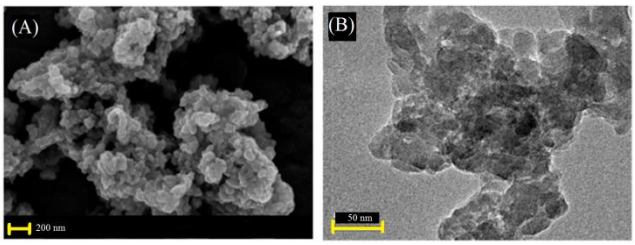


Fig. 3: Micrographs from washed Si nanoparticles synthesised with LiCl buffer: (A) SEM (B) TEM.

Morphological properties were analysed using images from both the TEM and SEM. Dispersing nanoparticles in a non-polar organic medium, such as toluene, is a major challenge as the particles tend to easily aggregate[23]. Toluene, however, does not contain any oxygen that could react with the sample, and was therefore used as a dispersing medium. A SEM image and a TEM image of washed Si sample synthesised using LiCl buffer are given in Fig. 3 (A) and (B). The images of the washed samples clearly show a high level of agglomeration, however, on close inspection, individual particles appear to be roughly spherical in nature.

It is difficult to gauge the size of the individual particles due to the high level of agglomeration, despite ultrasonication of the sample during preparation. However, there does appear to be a greater number of smaller Si particles in the sample prepared with buffer.

SAXS was employed to provide a more statistically meaningful size analysis of the nanoparticles. SAXS was performed on both washed samples to measure particles size for reactions without and with LiCl buffer (Eqn. 2) (Fig. 4). The data were radially integrated, background subtracted and processed to an absolute scale. The *Irena* software package[24] was used to model the particle size using a Unified Model approach. This model is described in detail in Beaucage[25] and divides the data obtained from SAXS into a series of Guinier regions and higher-*q* power laws to describe the sample morphology. Using this model with the assumption of spherical particles, an average particle diameter of 51 nm was determined for the sample without buffer and 13 nm for the sample with buffer. It is possible that there are also larger Si particles outside of the *q*-range of the SAXS measurements (i.e. > 60 nm) and the buffered sample displays evidence for this in TEM and from the presence of a low-*q* power law from surface scattering of larger particles.

## 4. Conclusion

Amorphous Si nanoparticles with tunable particle size, controlled using an inert buffer, were synthesised using liquid-solid mechanochemical synthesis for the first time. XRD was utilised to detect the presence of amorphous Si. SEM and TEM techniques, EELS and EFTEM, were used to map the morphology of the Si nanoparticles and suggest that the particles are roughly spherical with undetectable oxide levels. The Unified Fit modelling from SAXS data provides evidence for very small nanoparticles existing in large samples with sizes

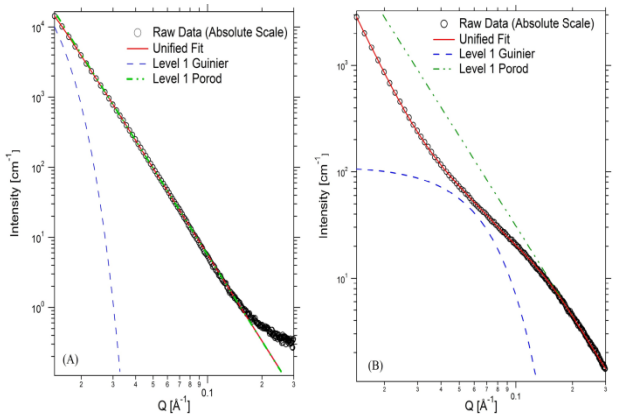


Fig. 4: Unified fit model to SAXS data from Si nanoparticles synthesised (A) without buffer (B) with buffer.

of 51 nm for Si synthesised without additional buffer and 13 nm for Si synthesised with buffer. Mechanochemical synthesis is an ideal technique to form small amorphous Si nanoparticles that have a range of technological applications.

## Acknowledgements

The authors acknowledge the financial support of the Australian Research Council (ARC) for ARC Linkage grant LP120101848. ARC LIEF grant LE0775551, and ARC RIEF grant R00107962, and the facilities, and the scientific and technical assistance of the Australian Microscopy & Microanalysis Research Facility at the Centre for Microscopy, Characterisation & Analysis, The University of Western Australia, a facility funded by the University, State and Commonwealth Governments.

[a] *Department of Imaging and Applied Physics, Fuel and Energy Technology Institute, Curtin University*
[b] *Institute of Materials Research, Materials Technology, Helmholtz-Zentrum Geesthacht, Max-Planck-Strasse 1, D-21502 Geesthacht, Schleswig-Holstein, Germany, email: anna-lisa.chaudhary@hzg.de*
[c] *Centre for Microscopy Characterisation and Analysis, The University of Western Australia, Crawley, WA 6009, Australia*

## References

1. S. Feng, D. Yu, H. Zhang, Z. Bai and Y. Ding, *J. Cryst. Growth*, 2000, **209**, 513 – 517.
2. Y. Kanemitsu, *J. Lumin.*, 2002, **100**, 209 – 217.
3. J. J. Vajo, F. Mertens, C. C. Ahn, R. C. Bowman and B. Fultz, *J. Phys. Chem. B*, 2004, **108**, 13977 – 13983.
4. A. C. Gangal, P. Kale, R. Edla, J. Manna and P. Sharma, *Int. J. Hydrogen Energy*, 2012, **37**, 6741 – 6748.
5. M. Paskevicius, D. A. Sheppard, A. L. Chaudhary, C. J. Webb, E. M. A. Gray, H. Y. Tian, V. K. Peterson and C. E. Buckley, *Int. J. Hydrogen Energy*, 2011, **36**, 10779-10786.
6. J. Bystrzycki, M. Polanski and T. Plocinski, *J. Nanosci. Nanotechnol.*, 2009, **9**, 3441 – 3448.
7. D. A. Sheppard, M. Paskevicius and C. E. Buckley, *J. Alloys Compd.*, 2010, **492**, L72 – L74.
8. A.-L. Chaudhary, D. A. Sheppard, M. Paskevicius, C. J. Webb, E. M. Gray and C. E. Buckley, *The Journal of Physical Chemistry C*, 2014, **118**, 1240-1247.
9. M. Paskevicius, D. A. Sheppard and C. E. Buckley, *J. Alloys Compd.*, 2009, **487**, 370 – 376.

 

10. C. Lam, Y. Zhang, Y. Tang, C. Lee, I. Bello and S. Lee, *J. Cryst. Growth*, 2000, **220**, 466 – 470.
11. A. C. Dodd and P. G. McCormick, *Scripta Mater.*, 2001, **44**, 1725 – 1729.
12. M. Paskevicius, Curtin University of Technology, 2009.
13. E. H. Zhou, C. Suryanarayana and F. H. Fores, *Mater. Lett.*, 1995, **23**, 27 – 31.
14. M. P. Pitt, M. Paskevicius, C. J. Webb, D. A. Sheppard, C. E. Buckley and E. M. Gray, *International Journal of Hydrogen Energy*, 2012, **37**, 4227-4237.
15. C. Maitland, Buckley, C.E., Paglia G. and Connolly, J., in *Proceedings of the Asia Pacific Nanotechnology Forum 2003 – OZ NANO 03*, World Scientific Publishing Co. Pty. Ltd, Cairns, Australia, Editon edn., 2004, pp. 113 – 120.
16. *CRC Handbook of Chemistry and Physics*, 74 edn., CRC Press, Inc., United States of America, 1994.
17. J. Wang, S. Ganguly, S. Sen, N. D. Browning and S. M. Kauzlarich, *Polyhedron*, 2013, **58**, 156-161.
18. Z. Wronski, R. A. Varin, C. Chiu, T. Czujko and A. Calka, *J. Alloys Compd.*, 2007, **434 – 435**, 743 – 746.
19. T. D. Shen, C. C. Koch, T. L. McCormick, R. J. Nemanich, J. Y. Huang and J. G. Huang, *J. Mater. Res.*, 1995, **10**, 139 – 148.
20. C. M. Poffo, J. C. de Lima, S. M. Souza, D. M. Triches, T. A. Grandi and R. S. de Biasi, *Journal of Raman Spectroscopy*, 2010, **41**, 1606 – 1609.
21. C. Ahn and O. Krivanek, *EELS atlas*, Gatan, 1983.
22. D. B. Williams, Carter, C. Barry, , *Transmission Electron Microscopy A Textbook for Materials Science* Boston, MA : Springer US, Boston, MA, 2009.
23. A. Reindl, A. Voronov, P. Gorle, M. Rauscher, A. Roosen and W. Peukert, *Colloids and Surfaces A: Physicochemical and Engineering Aspects*, 2008, **320**, 183 – 188.
24. J. Ilavsky and P. R. Jemian, *Journal of Applied Crystallography*, 2009, **42**.
25. G. Beaucage and D. W. Schaefer, *J. Non-Cryst. Solids*, 1994, **172 – 174, Part 2**, 797 – 805.